TISSUE ENGINEERING: Part C
Volume 19, Number 2, 2013
© Mary Ann Liebert, Inc.
DOI: 10.1089/ten.tec.2011.0629

Effect of Oxygen Concentration on Viability and Metabolism in a Fluidized-Bed Bioartificial Liver Using ^{31}P and ^{13}C NMR Spectroscopy

Rex E. Jeffries, PhD,[1] Michael P. Gamcsik, PhD,[1] Kayvan R. Keshari, PhD,[1] Peter Pediaditakis, PhD,[1] Andrey P. Tikunov, PhD,[1] Gregory B. Young, PhD,[2] Haakil Lee, PhD,[1] Paul B. Watkins, MD,[3] and Jeffrey M. Macdonald, PhD[1]

Many oxygen mass-transfer modeling studies have been performed for various bioartificial liver (BAL) encapsulation types; yet, to our knowledge, there is no experimental study that directly and noninvasively measures viability and metabolism as a function of time and oxygen concentration. We report the effect of oxygen concentration on viability and metabolism in a fluidized-bed NMR-compatible BAL using *in vivo* ^{31}P and ^{13}C NMR spectroscopy, respectively, by monitoring nucleotide triphosphate (NTP) and ^{13}C-labeled nutrient metabolites, respectively. Fluidized-bed bioreactors eliminate the potential channeling that occurs with packed-bed bioreactors and serve as an ideal experimental model for homogeneous oxygen distribution. Hepatocytes were electrostatically encapsulated in alginate (avg. diameter, 500 μm; 3.5×10^7 cells/mL) and perfused at 3 mL/min in a 9-cm (inner diameter) cylindrical glass NMR tube. Four oxygen treatments were tested and validated by an in-line oxygen electrode: (1) 95:5 oxygen:carbon dioxide (carbogen), (2) 75:20:5 nitrogen:oxygen:carbon dioxide, (3) 60:35:5 nitrogen:oxygen:carbon dioxide, and (4) 45:50:5 nitrogen:oxygen:carbon dioxide. With 20% oxygen, β-NTP steadily decreased until it was no longer detected at 11 h. The 35%, 50%, and 95% oxygen treatments resulted in steady β-NTP levels throughout the 28-h experimental period. For the 50% and 95% oxygen treatment, a ^{13}C NMR time course (~5 h) revealed 2-^{13}C-glycine and 2-^{13}C-glucose to be incorporated into [2-^{13}C-glycyl]glutathione (GSH) and 2-^{13}C-lactate, respectively, with 95% having a lower rate of lactate formation. ^{31}P and ^{13}C NMR spectroscopy is a noninvasive method for determining viability and metabolic rates. Modifying tissue-engineered devices to be NMR compatible is a relatively easy and inexpensive process depending on the bioreactor shape.

Introduction

In the field of bioartificial liver (BAL) tissue engineering, there has been a plethora of publications and interest in optimizing oxygen concentration for maintenance of long-term liver functions.[1–8] NMR spectroscopic analysis of BALs permit noninvasive quantification of viability and metabolic functions.[9] In conjunction with a fluidized-bed bioreactor, thorough mixing of oxygen within the perfusion chamber eliminates stagnant zones insuring oxygen homogeneity.[8,10] Therefore, in this study, we combine these two technologies to determine the effect of oxygen in a well-mixed fluidized bed. We determined viability and metabolic rates by noninvasively monitoring ATP levels and biotransformation of 13C-labeled nutrients, respectively, via *in vivo* ^{31}P and ^{13}C NMR spectroscopy, respectively.

Physiological oxygen concentration across the liver decreases from 0.13 mM (equivalent to the oxygen medium concentration achieved by gas exchange with a 13% oxygen mixture) to just above 0.04 mM (achieved with 4% oxygen mixture),[11] while metabolic enzyme activity tracks this oxygen gradient.[12] However, in two-dimensional (2D) hepatocyte cultures, the oxygen concentration is near 0.2 mM by using exchange with air (20% oxygen) via the cell culture vessel's headspace. Carbogen, a 95% mixture of oxygen with 5% carbon dioxide, is often used in three-dimensional (3D) BALs. Conventionally, 95% oxygen mixtures are used for perfused liver studies,[13] an extension of the first perfused organ studies performed by Langendorf.[14] Survival of hepatocytes at these low oxygen tensions (0.4–0.13 mM) *in vivo* is likely due to relatively small diffusion distances (0.05 mm or less) and the presence of hemoglobin, which buffers the

Departments of [1]Biomedical Engineering, and [2]Biochemistry and Biophysics, University of North Carolina at Chapel Hill, Chapel Hill, North Carolina.
[3]Hamner-UNC Institute for Drug Safety Sciences, Research Triangle Park, North Carolina.

oxygen load in blood nearly two orders of magnitude.[13] Historically, 3D membrane-type BAL studies have used higher oxygen levels in media to traverse the larger diffusion distances without the aid of oxygen carriers,[9,15–19] whereas lower oxygen concentrations have been used with microcarrier[20–22] and flatbed[1,3,10,23–25] BAL designs, where the majority of hepatocyte reside at the medium–surface interface. The encapsulate type of BALs have seen a full range of oxygen concentrations used, making this category the most variable in terms of oxygen concentration in the literature.[8,10,26–28]

In this work, a fluidized-bed NMR-compatible bioreactor is used that contains alginate-encapsulated hepatocytes at a density of 3.5×10^7 cell/mL. The alginate encapsulates are produced with a 250-μm uniform spherical radius, which is the maximal distance that will not create a hypoxic core, using cell and oxygen concentrations in the media typical of BAL studies.[7,28] The fluidized-bed bioreactor creates a constant free fall of the encapsulates,[8] by percolating them, and insuring homogenous perfusion, thereby achieving robust nutrient mass transfer, so that the dependent variable, oxygen concentration in the perfusion media, can be reliably tested. Four oxygen treatments (95%, 50%, 35%, and 20%) were tested for maintaining viability using *in vivo* ^{31}P NMR spectroscopy to noninvasively monitored β-nucleotide triphosphate (NTP) levels, a direct measure of viability.[9,29,30] *In vivo* ^{13}C NMR spectroscopy noninvasively monitored metabolism of 4 mM 2-^{13}C-glycine, 4 mM U-^{13}C-glutamine, and 25 mM 2-^{13}C-glucose, which replaced their ^{12}C analog in the media. The oxygen levels used in this study span those used in the literature[8,10,26–28] and are used to demonstrate the use of the noninvasive NMR spectroscopy methodology, as it relates to BAL research and development.

Materials and Methods

Overall study design

Four oxygen treatments were tested to determine their effect on viability using *in vivo* ^{31}P NMR spectroscopy. The gas mixtures were (1) 95:5 oxygen:carbon dioxide (i.e., carbogen), (2) 75:20:5 nitrogen:oxygen:carbon dioxide, (3) 60:35:5 nitrogen:oxygen:carbon dioxide, and (4) 45:50:5 nitrogen:oxygen:carbon dioxide. Oxygen concentrations were empirically determined for each treatment using oxygen electrodes placed inside the bioreactor in separate benchtop experiments and correlated to the NMR experiment. The bioreactor[31,32] life-support unit, including the gas exchange unit that also acts to heat the media before entry into the NMR spectrometer, was previously described in earlier work,[33] and in more detail below. In the two highest oxygen treatments, 50% and 95%, the *in vivo* ^{13}C NMR spectroscopy studies were demonstrated.

Materials

NMR supplies were obtained from multiple vendors. Sodium alginate, calcium chloride, perchloric acid, sodium citrate, sodium chloride, potassium chloride, magnesium sulfate, 4-(2-hydroxyethyl)-1-piperazineethanesulfonic acid (HEPES), bovine serum albumin (BSA), and 3-(trimethylsily)propionic-2,2,3,3-d_4 acid (TSP) were purchased from Sigma Chemical company (St. Louis, MO). Mono- and dibasic phosphate were purchased from Mallinckrodt (Paris, KY). Dulbecco's Modified Eagle's Medium, insulin, penicillin, streptomycin, and fetal bovine serum were purchased from Invitrogen, Inc. (Carlsbad, CA). For the Clark electrode, saturated potassium chloride solution was purchased from Mettler Toledo AG (Schwerzenbach, Switzerland), and silver and platinum wire was purchased from Goodfellow Corp. (Oakdale, PA). The 2+1 channel PC digital oscilloscope (DS1M12 Stingray) with accompanying software was purchased from USB Instruments (Hillsboro, OR). Deuterium oxide was from Cambridge Isotope Laboratories (Andover, MA). The 5- and 10-mm NMR tubes were purchased from Wilmad Labglass, Inc. (Miamisburg, OH), while Norprene™ and Silastic™ tubing, tube connector, peristaltic pump were from Cole Parmer (Vernon Hills, IL). The water bath and 500-mL Gibco™ reservoir culture bottles were from Fisher (Pittsburgh, PA). Bioreactor end pieces were manufactured from Delrin™ and assembled as previously described.[31,32] Materials for the bioreactor life-support units were described in earlier work.[33]

Bioreactor design and life support system

Alginate-encapsulated hepatocytes were perfused in a 10-mm screw-cap NMR tube (Fig. 1). A Delrin™ fixture provided aseptically sealed input and output ports. The encapsulated cells were retained in the BAL by a fabricated

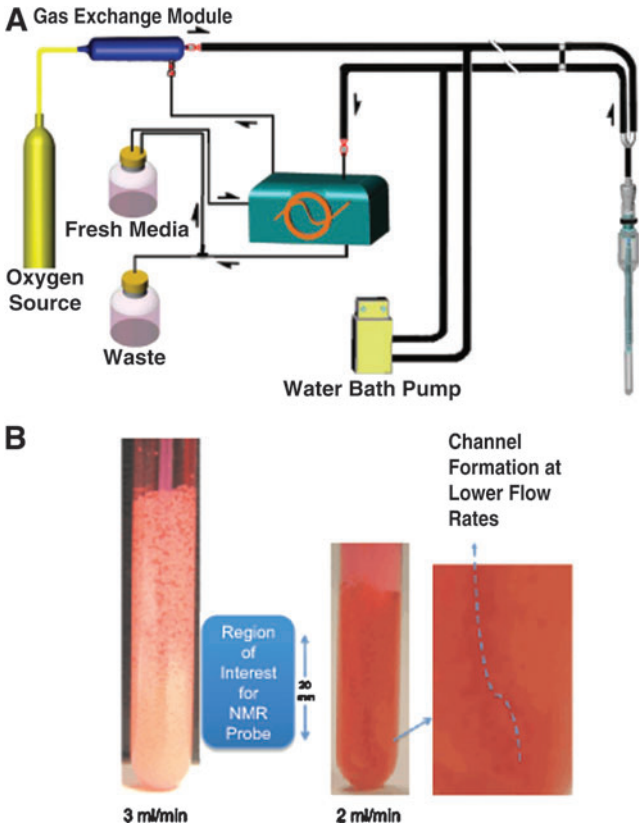

FIG. 1. A schematic diagram of the bioreactor life-support loop and the bioreactor: block diagram of the bioreactor loop **(A)**. Close-up picture of the bioreactor with encapsulates—in action **(B)**. See Supplementary Data for the video of the bioreactor at two flow rates, 2 and 3 mL/min. Color images available online at www.liebertpub.com/tec

finned baffle with 300-μm holes. FEP Teflon® tubing (0.8-mm inner diameter (I.D.) × 1.6-mm outer diameter (O.D.); Cole Parmer) was used to transport the medium to the bottom of the NMR tube. A second FEP Teflon line (1.6-mm I.D. × 3.2-mm O.D) was used to remove the medium above the end piece. To maintain the temperature at 37°C, both the input and output lines were water jacketed with Norprene® tubing (9.525-mm I.D. × 15.875-mm O.D.; Cole Parmer).

Perfusion medium oxygenation was provided with a previously described[33] gas-exchange module. Clark electrodes for dissolved oxygen measurements were fabricated from Delrin™ using platinum and silver wire, contained in a solution of saturated potassium chloride, positioned behind a semipermeable membrane as described in.[34] Two electrodes were located in the inlet and outlet lines and interfaced to a laptop computer through a 2 + 1 channel PC digital oscilloscope, a DS1M12 Stingray analog to digital converter. The recorded oxygen measurements were utilized to calculate the oxygen concentration in the various oxygen treatments. The culture medium was recirculated at 3 mL/min through the encapsulated cells with a peristaltic pump (Masterflex; Cole Parmer). A video of encapsulates perfused at two flow rates is given in the Supplementary Data (Supplementary Data are available online at www.liebertpub.com/tec).

Hepatocyte isolation procedure

All animals were housed and treated in accordance with the guidelines set by the Institutional Animal Use and Care Committee of the University of North Carolina. Sprague-Dawley rats (Charles Rivers, Frederick, MD) were housed with a 12-h dark cycle and allowed water and food *ad libitum*. The rats were anesthetized with Nembutal (0.5 μg/g body weight), and the hepatocytes were isolated following a two-step collagenase perfusion of the liver.[35] After isolation, the hepatocytes were incubated at 37°C in Krebs-Ringer-HEPES (KRH) (116 mM NaCl, 5 mM KCl, 1 mM KH_2PO_4, 2.5 mM $MgSO_4$, 2.5 mM $CaCl_2$, 25 mM HEPES, 1% BSA, pH 7.4) for 10 min. While at 37°C, the cells were gently mixed every 2 min. Next, the hepatocytes were settled for 15 min on ice, and the top layer was removed. Lastly, the cells were washed in KRH and pelleted at 50 × *g* three times. After the final spin, the hepatocytes were resuspended in KRH, and the cell number and viability were assessed by trypan blue exclusion.

Encapsulation methods, inoculation of the bioreactor, and recapture of hepatocytes

Cells were encapsulated using an electrostatic encapsulate generation apparatus described previously[36] with modifications.[31] Briefly, rat hepatocytes at a density of 7×10^7 cells/mL were suspended in a 2% sodium alginate solution at a 1:1 ratio. The resulting 1% alginate solution containing 3.5×10^7 cells/mL was put in a 1-cc syringe fitted with a 24-gauge angiocatheter. The angiocatheter was pierced at the hub with a 27-gauge needle, which served as the positive electrode for the electrostatic casting process. The syringe was placed in a syringe pump (Braintree Scientific BS-8000, Braintree, MA) and arranged such that as droplets were ejected from the angiocatheter, they would fall orthogonally into the 150 mM $CaCl_2$ saline solution bath (6.7 mM KCl, 142 mM NaCl, HEPES 10 mM at pH 7.4) at 4°C. Encapsulates were transferred to the culture medium within 2 min to avoid excessive exposure to calcium. The distance from the angiocatheter tip to the surface of the $CaCl_2$ solution was fixed at 2.5 cm. The pump flow rate was set within the range of 0.75 to 1.5 mL/min. A grounded electrode was immersed in the $CaCl_2$ receiving bath. When the syringe pump was turned on, in the presence of the high electrostatic potential (~6 kV), the sodium alginate solution was pulled away from the angiocatheter tip as tiny droplets that polymerize into solid calcium alginate immediately upon contact with the $CaCl_2$ saline. The bioreactor was inoculated with 1.5 mL of encapsulates ($\sim 5.3 \times 10^7$ cells) and capped, and perfusion started immediately. A flow rate of 3 mL/min was chosen, because this was the maximum to maintain a convective free fall of the encapsulates without packing them on the baffles and clogging the exit ports. A video of encapsulates perfused at two flow rates, 3 mL/min versus 2 mL/min, demonstrates that 3 mL/min is the optimum flow rate, and are in the Supplementary Data. The time from the end of hepatocyte isolation to inoculation was < 3 h. Although *in vivo* ^{31}P NMR spectroscopic monitoring of NTP levels is a validated measure of viability,[29] viability was assessed by trypan blue exclusion for the 95% oxygen treatment at the end of the experiment, just to confirm this method with the gold standard in the field. The hepatocytes were recaptured from the alginate encapsulates by addition of 100 mM citrate in phosphate-buffered saline (PBS), centrifuged, and rinsed with PBS, and the dissolved alginate was aspirated before trypan blue addition, and the viability was determined using a hemocytometer.

In vivo *^{31}P and ^{13}C NMR spectroscopy*

In vivo ^{31}P NMR experiments of the primary rat hepatocytes were performed on a narrow-bore 14.1T (600 MHz ^{1}H frequency) Varian INOVA NMR spectrometer equipped with a 10-mm-broadband probe (Venus Probes, Livermore, CA). The receiver frequency of the probe was tuned to ^{31}P at 242.78 MHz and ^{13}C at 150.92 MHz. For ^{31}P NMR spectroscopy, a one-pulse sequence with a sweep width of 10,000 Hz and 16 K complex data points, using a calculated Ernst angle of 77° (22 μs) and a 2-s repetition time. A total of 668 transients resulted in 34-min spectra for the ^{31}P NMR spectral time course, and to increase signal to noise, at least four spectra are summed for determining the peak areas. For ^{13}C one-pulse sequence with ^{1}H decoupling during acquisition with GARP-1, and using a sweep width of 40,000 Hz and 16 K complex data points, using a flip angle of 60°, with a 2 s repetition time. The ^{31}P NMR data were processed off-line with ACD/Specmanager software (ACD/Labs, Toronto, Ontario, Canada) with 60-Hz line broadening. The signal-to-noise function in ACD software was used to calculate the signal-to-noise ratio (SNR) of the ß-NTP peak in the various *in vivo* ^{31}P NMR spectra using a downfield region (~10 to 12 ppm) to calculate the noise level. ^{31}P metabolites were identified using α-NTP (−7.5 ppm) as an internal reference. The *in vivo* ^{31}P NMR spectra were peak-fitted using the Gauss-Lorentz apodization and plotted as ratios of their absolute peak area at each time point relative to the peak area of the external phosphate peak. The *in vivo* ^{31}C NMR spectral time courses were converted to concentration time

courses for lactate by calibrating the peak areas of the C2 of lactate at each spectral time point to the peak area of medium glucose from the first spectrum in the time course to 25 mM/L, multiplying by the loop volume (L), and then dividing by the number of hepatocytes inoculated, resulting in nmol per million hepatocytes. These data points plotted over the time course, and then fit with a linear equation, $y = Ax + B$, to obtain the lactate production rates. We have previously shown that lactate production rates in lactate-depleted media are linear in hepatocyte cultures.[37] The lactate levels were validated in the 95% oxygen treatment studies using the UNC Animal Clinical Chemistry and Gene Expression Core Facility's Johnson & Johnson's VT350 Automatic Chemical Analyzer.

Results

Figure 1 is a schematic of the bioreactor loop and bioreactor (Fig. 1A) with a close-up picture of the bioreactor with encapsulates during perfusion demonstrating the suspension of encapsulates and their homogeneous diameter (Fig. 1B). See Supplementary Data for a video of the perfused encapsulates at different flow rates. In this suspension, encapsulates are perfused at a rate that causes them to percolate, avoiding both stagnation and channeling. The flow rate is adjusted such that encapsulates are kept within a fixed volume and a closed perfusion loop. The fluidization of encapsulates results from the density difference between encapsulates and fluid, and the closed loop creates back-pressure and gravity, which counters the upward velocity of the laminar fluid flow causing convection of the encapsulates.[8]

Figure 2 depicts stack plots of the time course of *in vivo* ^{31}P NMR spectra of encapsulated rat hepatocytes perfused with 20%, 35%, 50%, and 95% oxygen from $t = 0$ (bottom) to $t = 12$, 27, 20, and 25 h, respectively. The ^{31}P NMR spectra required 68 min to acquire and permits noninvasive quantification of the three peaks representing NTP (in the liver, ATP is about 80% of NTP[38]), medium phosphate (Pi_e), intracellular phosphate (Pi_i), oxidized plus reduced nicotinamide adenine dinucleotide, diphosphodiesters like UDP-glucose, sugar phosphates mostly related to glycolysis, and phospholipid intermediates such as phosphocholine, phosphoethanolamine, glycerophosphocholine, and glycerophosphoethanolamine. The 20% oxygen treatment β-NTP levels never recovered from the isolation process, whereas the 35%, 50%, and 95% oxygen treatments maintained β-NTP levels throughout the experimental period (Fig. 2). Similar to the 20% oxygen treatments (time course not shown), the sugar phosphates were relatively elevated in the 95% oxygen treatment (visible in Fig. 2A), but disappeared within several hours of perfusion. The spectral SNR was the best for 95% oxygen treatment with a value of 8.1 for β-NTP at 5 h (second spectrum Fig. 2D), whereas it was 5.9 and 4.9 for 50% and 35% oxygen treatment, respectively (second spectra Fig. 2C, B).

Figure 3 shows that 35%, 50%, and 95% oxygen treatments maintained viability over the experimental period, and achieved our goal of maintaining hepatocyte viability for at least 24 h. The β-NTP levels increased slowly for 50% and 35%, reaching 122% ± 3% and 118%, respectively, by 10 h, whereas it was fairly constant throughout the 95% oxygen treatment. The viability was determined at the end of the experiment in the 95% oxygen treatment by trypan blue and was 82% ± 5%, which was comparable to the starting value of

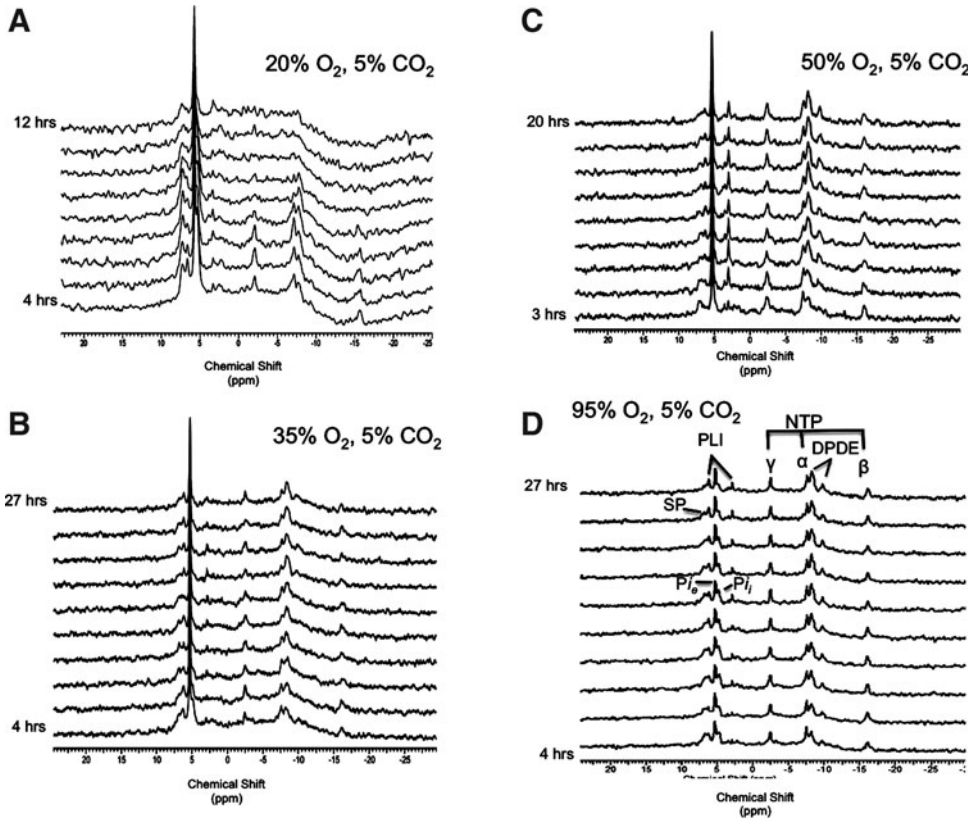

FIG. 2. Stack plot of *in vivo* ^{31}P NMR spectral time course of encapsulated rat hepatocytes perfused with **(A)** 20% from 0 to 12 h, **(B)** 35% from 0 to 27 h ($n = 2$) **(C)** 50% from 0 to 20 h ($n = 2$), and **(D)** 95% oxygen from 0 to 27 h ($n = 2$). Each ^{31}P NMR spectrum required 68 min to acquire showing every spectrum for the 20% oxygen treatment, and every other spectrum for the other oxygen treatments. NTP, nucleotide triphosphate; DPDE, diphosphodiester; NAD(H), reduced and oxidized nicotinamide adenine dinucleotide; PLI, phospholipid intermediates; Pi_i, intracellular phosphate; Pi_e, extracellular phosphate; SP, sugar phosphates.

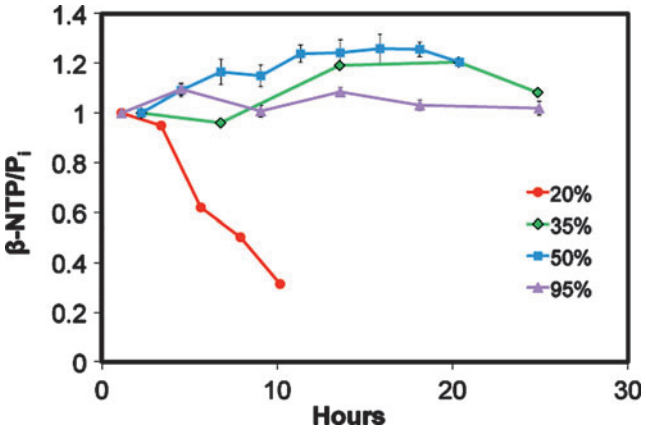

FIG. 3. Graphs of β-NTP/Pi from hepatocytes perfused with media subjected to 20% ($n=1$), 35% ($n=2$), 50% ($n=2$), and 95% ($n=2$) oxygen. Color images available online at www.liebertpub.com/tec

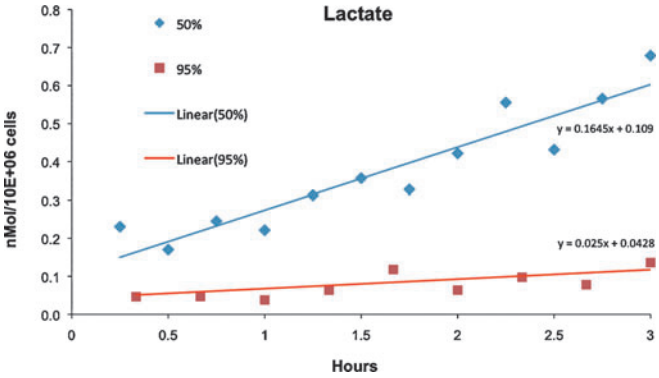

FIG. 5. The *in vivo* lactate time courses of the 50% and 95% oxygen treatments. Lactate production rate for the 50% and 95% oxygen treatments is 45.69 pM/10^6 cells/s and 6.94 pM/10^6 cells/s, respectively. Color images available online at www.liebertpub.com/tec

89%±4%. The 20% oxygen treatment caused a steady decrease from the start of *in vivo* ^{31}P NMR spectroscopy acquisition with the β-NTP peak not detectable by 10 h.

To test metabolic function, the ^{13}C NMR spectroscopy time course was run for the two highest oxygen concentrations, 50% and 95%, by following the metabolism of 25 mM 2-^{13}C-glucose, 4 mM U-^{13}C-glutamine, and 4 mM 2-^{13}C-glycine replaced in the media for their ^{12}C analog. Figure 4 is an *in vivo* ^{13}C NMR spectrum of hepatocytes perfused with media supplied 50% oxygen from 22 to 25.5 h of postinoculation. The spectral time course is shown (inset) for the glucose (Fig. 4A), lactate (Fig. 4B), and glutathione (GSH) (Fig. 4C) resonances. Figure 5 is the *in vivo* lactate time courses of the 50% and 95% oxygen treatment, showing that the rate of lactate production, an end product of anaerobic glycolysis, is lower in the 95% oxygen treatment. The production rate of lactate for the 50% and 95% oxygen treatments is 45.69 pmol/10^6 cells/s and 6.94 pmol/10^6 cells/s, respectively. The GSH rate was not calculated as it typically

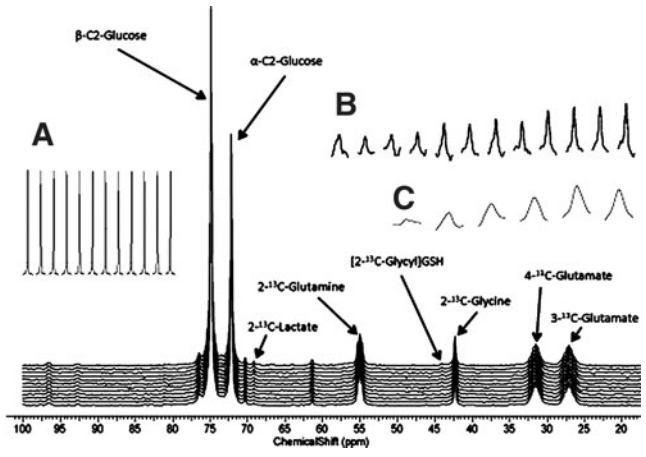

FIG. 4. An *in vivo* ^{13}C NMR spectrum of hepatocytes perfused with media supplied 50% oxygen from 22 to 25.5 h of postinoculation; **(A)** glucose, **(B)** lactate, and **(C)** glutathione (GSH).

requires 7–12 h to reach isotopic steady state in rat liver,[39] but the relative incorporation per 10^6 cells is slightly greater in the 95% as compared to the 50% oxygen treatment.

Discussion

Although BAL technology was first introduced three decades ago,[4] the optimum oxygen concentration to use for encapsulation-type or membrane-type BALs remains unclear and is often BAL specific. Langendorf[14] initially used a 95% oxygen mixture in his perfused heart studies, and this has remained the standard for tissue engineering for the majority of perfused membrane-type BALs, while 3D encapsulation-type BALs[8,10,26,27,40] and organoid constructs[41,42] have varied. Hepatocytes are highly aerobic, requiring high amounts of oxygen relative to other tissues. *In vivo*, the oxygen-carrying capacity of hemoglobin increases oxygen concentration nearly two orders of magnitude and maintains an oxygen gradient across the acinus from 0.13 mM (equivalent to 13% oxygen) to 0.04 mM (equivalent to 4% oxygen) where blood exits the liver.[4] To date, there is no publication on a NMR-compatible BAL describing the viability and longevity of hepatocytes using ^{31}P NMR concomitant with metabolic rates using ^{13}C NMR in response to systematic increments of oxygen concentration in the perfusate.

According to our data, these cells administered physiological levels of 20% oxygen would have died at ~10 h after inoculation in the bioreactor likely due to hypoxia, while those given >34% oxygen survived (Fig. 3), with rates of glycolytic end products faster in lower oxygen concentration, whereas levels of antioxidant synthesis were faster in higher oxygen concentration (Fig. 5). Since oxygen levels between 20% and 35% were not tested, the precise threshold oxygen level for survival was not determined, and these results can only be extrapolated to 9-mm-diameter fluidized bioreactor containing about 7×10^7 hepatocytes with a flow rate of 3 mL/min.

Oxygen concentrations in perfusion media and NMR-compatible BAL viability and function

For 20% oxygen treatment and a 500-μm diameter used in this study, there would be a hypoxic core (<3%),[43] perhaps explaining the continuous loss of β-NTP (Fig. 3). In fact, in

hepatocyte spheroids of 500-μm diameter and given 20% oxygen, there was only 60% viability at 60 μm from the surface exponentially decreasing to 10% viability at 250 μm from the surface.[43] The radius of encapsulates used in this study is 250 μm with cell densities of 0.35×10^7 cells/mL, unlike the aforementioned study,[43] which modeled hepatocyte spheroids closer to a tissue density of 2.5×10^8 cells/mL[4]; therefore, direct comparison to this study cannot be made. An NMR-compatible BAL study, using a coaxial membrane bioreactor, compared two bioreactors with 200- and 500-μm diffusion distance and found that only the former bioreactor maintained viability with 95% oxygen.[17] An oxygen mass-transfer study of collagen-encapsulated hepatocytes at 35-fold less cell density than the present study found that 170 μm is the maximum diffusion distance beyond which the hypoxic condition exists.[44]

A diameter of 500 μm can replicate the oxygen gradient of 13% in the portal triad and decreasing to 4% near the portal vein, a distance of 500 μm.[11] The oxygen gradient across the acinus controls metabolic functions.[45] Short -term[46] and long -term[47] 2D culture of rat hepatocytes have demonstrated that these functions are replicated using 13% and 4% oxygen, with glycolysis the primary bioenergetic process at 4% oxygen. These oxygen-driven metabolic functions could be replicated across the encapsulate, mimicking the gradient of function across the acinus. However, hemoglobin contained in red blod cells traverses the 500-μm acinar distance holding over 70-fold more oxygen in the same volume acting as an oxygen buffer.[4] Oxygen carriers were not included in the alginate encapsulate. To increase metabolic rates in BALs, recently Yangi and Ohshima[5] compared 10%, 20%, 30%, and 40% oxygen level in 2D rat hepatocyte cultures and found that 40% oxygen treatment resulted in the highest urea and albumin production rates at days 2 and 4. Use of 95% oxygen causes hyperoxic concentrations resulting in a more rapid hepatocyte death in 2D suspension cultures than 20% oxygen, or air.[48] In a perfused liver treated with 84% oxygen (640 mmHg oxygen in the perfusate), the cause of cell damage is due to oxidative stress resulting from reactive oxygen species generated from the elevated oxygen concentration in the perfusate.[49] Our results of 35%, 50%, and 95% oxygen seem to corroborate the findings of Yanagi and Ohshima,[5] whereby relatively higher oxygen tensions are required for optimal 3D BAL performance, at least for diffusion distances of 250 μm tested in the alginate encapsulates. Although the oxygen gradient is steeper across the encapsulates than the acinus, the 500-μm-diameter encapsulate in conjunction with a cell density used in this study and oxygen levels >34% result in oxygen levels in the range of what is tolerated by rat hepatocytes.[5,45–47,50]

In vivo ^{13}C NMR spectroscopy: metabolism in 50% and 95% oxygen treatments

NMR spectroscopy can provide noninvasive analysis metabolic rates. Lactate production is an end product of anaerobic glycolysis and a measure of hypoxia. Lactate is produced primarily in the periportal region in the less-mature cells of the acinus,[4,45] and was found in perfuse rat livers to decrease in response to ammonia ranging from 633–917 pmol/s/mL of tissue volume and assuming 2.5×10^8 hepatocytes/mL tissue, that is, 2.5–3.7 pmol/10^6 cells/s[51] and 8.5 pmol/10^6 cells/s. In a rotary culture BAL consisting of hollow fiber and inoculated with small human hepatocytes perfused with medium oxygenated with 95% oxygen, the lactate production rate was 53 pmol/10^6 cells/s.[52] Our results show that the higher oxygen rates demonstrated lower lactate production rates 6.9 pmol/10^6 cells/s. This is in line with oxygenation throughout the encapsulate, without a hypoxic core, in the 95% oxygen treatment, which is supported by mass-transfer models.[43,44] Although the 50% oxygen level resulted in a higher lactate production rate 45.7 pmol/10^6 cells/s, it is significantly lower than a rat hepatoma cell line encapsulated and perfused in the same bioreactor, but perfused with 20% oxygen (i.e., air), which was 121.2 pmol/10^6 cells/s. The more elevated lactate production occurs in transformed hepatocytes in the these BAL publications, likely due to the Warburg effect[54]; however, the 2D cultures of rat hepatocytes and perfused rat liver lactate production rates are closer in a range to that of the 95% oxygen treatment. It possible that the difference between the 50% oxygen treatments to that of the 21% oxygen treatment could be due to a hypoxic core, or there is a higher proportion of the periportal zone-1 hepatocytes, which have higher rates of lactate production,[47,53] which survived the isolation process and were used to inoculate the bioreactor.

Summary

In short, this is the first comprehensive *in vivo* ^{31}P NMR study of oxygen treatment of NMR-compatible BALs to determine a range of oxygen concentrations for long-term viable cultures. The 20% oxygen treatment did not maintain viability, but 35%, 50%, and 95% oxygen treatments maintained viability for the duration the experiment (~24 h). The higher oxygen treatment of 95% decreased lactate production rates to the range found in 2D culture of rat hepatocytes. *In vivo* $^{31}P/^{13}C$ NMR is an ideal noninvasive method to optimize operational parameters of BALs, once the BAL has been made NMR compatible.[9]

Acknowledgments

We thank NIH grants (GM075941, GM38149, P30ES010126 and CA114365) for funding the research. REJ was funded by a predoctoral NRSA (F31DK082172) in the last stage of this work. We appreciate the help of Kevin Keys for performing the histology, and Alisher Holmuhamedov and Ryan Webb for their assistance in constructing bioreactors and life-support units.

Disclosure Statement

No competing financial interests exist.

References

1. Bhatia, S.N., Toner, M., Tompkins, R.G., and Yarmush, M.L. Selective adhesion of hepatocytes on patterned surfaces. Ann N Y Acad Sci **745,** 187, 1994.
2. Catapano, G., De Bartolo, L., Lombardi, C.P., and Drioli, E. The effect of oxygen transport resistances on the viability and functions of isolated rat hepatocytes. Int J Artif Organs **19,** 61, 1996.
3. Ledezma, G.A., Folch, A., Bhatia, S.N., Balis, U.J., Yarmush, M.L., and Toner, M. Numerical model of fluid flow and

oxygen transport in a radial-flow microchannel containing hepatocytes. J Biomech Eng **121,** 58, 1999.
4. Macdonald, J.M., Griffin, J., Kubota, H., Griffith, L., Fair, J., and Reid, L.M. Bioartificial livers. In: Kuhtreiber, W., Lanza, R.P., and Chick, W.L., eds. Cell Encapsulation Technology and Therapeutics. Cambridge, MA: Birkhauser Boston, 1999, pp. 252–286.
5. Yanagi, K., and Ohshima, N. Improvement of metabolic performance of cultured hepatocytes by high oxygen tension in the atmosphere. Artif Organs **25,** 1, 2001.
6. Allen, J.W., and Bhatia, S.N. Formation of steady-state oxygen gradients *in vitro*: application to liver zonation. Biotechnol Bioeng **82,** 253, 2003.
7. McClelland, R.E., MacDonald, J.M., and Coger, R.N. Modeling O2 transport within engineered hepatic devices. Biotechnol Bioeng **82,** 12, 2003.
8. David, B., Doré, E., Jaffrin, M.Y., and Legallais, C. Mass transfers in a fluidized bed bioreactor using alginate beads for a future bioartificial liver. Int J Artif Organs **27,** 284, 2004.
9. Jeffries, R.E., and Macdonald, J.M. New advances in MR-compatible bioartifical liver. Nmr Biomed **25,** 427, 2012.
10. Murtas, S., Capuani, G., Dentini, M., Manetti, C., Masci, G., Massimi, M., *et al.* Alginate beads as immobilization matrix for hepatocytes perfused in a bioreactor: a physico-chemical characterization. J Biomater Sci Polym Ed **16,** 829, 2005.
11. McCuskey, R.S. The hepatic microvascular system. In: Arias, I.M., Boyer, J.L., Fausto, N., Jakoby, W.B., Schachter, D.A., and Shafritz, D.A., eds. The liver: Biology and Pathobiology New York: Raven Press, 1994. pp. 1089–1106.
12. Gebhardt, R. Metabolic zonation of the liver: regulation and implications for liver function. Pharmacol Ther **53,** 275, 1992.
13. Catapano, G., Patzer, J.F., 2nd, and Gerlach, J.C. Transport advances in disposable bioreactors for liver tissue engineering. Adv Biochem Eng Biotechnol **115,** 117, 2010.
14. Langendorff, O. Neuere Untersuchungen über die Ursache des Herzschlages. Ergebnisse der Physiologie, biologischen Chemie und Experimentellen Pharmakologie **4,** 764, 1905.
15. Gerlach, J.C., Schnoy, N., Encke, J., Smith, M.D., and Müller, C.P.N. Improved hepatocyte *in vitro* maintenance in a culture model with woven multicompartment capillary systems: electron microscopy studies. Hepatology **22,** 546, 1995.
16. Flendrig, L.M., la Soe, J.W., Jörning, G.G.A., Steenbeek, A., Karlsen, O.T., Bovée WMMJ, *et al. In vitro* evaluation of a novel bioreactor based on an integral oxygenator and a spirally wound nonwoven polyester matrix for hepatocyte culture as small aggregates. J Hepatol **26,** 1379. 1997.
17. Macdonald, J.M., Grillo, M., Schmidlin, O., Tajiri, D.T., and James, T.L. NMR spectroscopy and MRI investigation of a potential bioartificial liver. NMR Biomed **11,** 55, 1998.
18. McClelland, R.E., and Coger, R.N. Effects of enhanced O(2) transport on hepatocytes packed within a bioartificial liver device. Tissue Eng **10,** 253, 2004.
19. Seagle, C., Christie, M.A., Winnike, J.H., McClelland, R.E., Ludlow, J.W., O'Connell, T.M., *et al.* High-throughput nuclear magnetic resonance metabolomic footprinting for tissue engineering. Tissue Eng Part C Methods **14,** 107, 2008.
20. Shnyra, A., Bocharov, A., Bochkova, N., and Spirov, V. Bioartificial liver using hepatocytes on biosilon microcamers: treatment of chemically induced acute hepatic failure in rats. Artif Organs **15,** 189, 1991.
21. Li, A.P., Barker, G., Beck, D., Colburn, S., Monsell, R., and Pellegrin, C. Culturing of primary hepatocytes as entrapped aggregates in a packed bed bioreactor: a potential bioartificial liver. In Vitro Cell Dev Biol **29A,** 249, 1993.
22. Schutte, M., Fox, B., Baradez, M.O., Devonshire, A., Minguez, J., Bokhari, M., *et al.* Rat primary hepatocytes show enhanced performance and sensitivity to acetaminophen during three-dimensional culture on a polystyrene scaffold designed for routine use. Assay Drug Dev Technol **9,** 475, 2011.
23. Uchino, J., Tsuburaya, T., Kumagai, F., Hase, T., Hamada, T., Komai, T., *et al.* A hybrid bioartificial liver composed of multiplated hepatocyte monolayers. ASAIO Proc **34,** 972, 1988.
24. De Bartolo, L., Jarosch-Von Schweder, G., Haverich, A., and Bader, A. A novel full-scale flat membrane bioreactor utilizing porcine hepatocytes: cell viability and tissue-specific functions. Biotechnol Prog **16,** 102, 2000.
25. Kusumi, T., Ishihara, K., Mizumoto, H., Nakazawa, K., Ijima, H., Funatsu, K., *et al.* Evaluation of a bioreactor with stacked sheet shaped organoids of primary hepatocytes. J Biosci Bioeng **107,** 552, 2009.
26. Takabatake, H., Koide, N., and Tsuji, T. Encapsulated multicellular spheroids of rat hepatocytes produce albumin and urea in a spouted bed circulating culture system. Artif Org **15,** 474, 1991.
27. Miccheli, A., Tomassini, A., Capuani, G., Di Cocco, M.E., Sartori, E., Falasca, L., *et al.* Energy metabolism and re-establishment of intercellular adhesion complexes of gel entrapped hepatocytes. Cytotechnology **32,** 219, 2000.
28. Ogbonna, J.C., Matsumura, M., and Kataoka, H. Effective oxygenation through reduction in bead diameters: a review of immobilized cells. Proc Biochem **26,** 109, 1991.
29. Mancuso, A., Fernandez, E.J., Blanch, H.W., and Clark, D.S. A nuclear magnetic resonance technique for determining hybridoma cell concentration in hollow fiber bioreactors. Biotechnology **8,** 1282, 1990.
30. Mancuso, A., and Glickson, J.D. Applications of NMR Spectroscopy and Imaging to the Study of Immobilised Cell Physiology, first edition. Norwell, MA: Kluwer Academic Publishers, 2004.
31. Jeffries, R., Keshari, K., Seagle, C., Pediaditakis, P., Gamcsik, M., Kurhanewicz, J., and Macdonald, J. A vesatile NMR-compatible bioreactor for alginate-encapsulated liver cells. Presented at the International Society for Magnetic Resonance in Medicine (ISMRM) 16th Scientific Meeting & Exhibition, Toronto, Ontario, Canada, 2008.
32. Keshari, K.R., Kurhanewicz, J., Wilson, D.M., Jeffries, R.E., Dewar, B.J., Van Criekinge, M., *et al.* Hyperpolarized 13C spectroscopy and a novel NMR-compatible bioreactor system for the investigation of real time cellular metabolism. Magn Reson Med **63,** 322, 2010.
33. Gamcsik, M.P., Forder, J.R., Millis, K.K., and McGovern, K.A. A versatile oxygenator and perfusion system for magnetic resonance studies. Biotechnol Bioeng **49,** 348, 1996.
34. Tikunov, A., Johnson, C.B., Pediaditakis, P., Markevich, N., Macdonald, J.M., Lemasters, J.J., *et al.* Closure of VDAC causes oxidative stress and accelerates the Ca(2+)-induced mitochondrial permeability transition in rat liver mitochondria. Arch Biochem Biophys **495,** 174, 2010.
35. Jirtle, R.L., Michalopoulos, G., McLain, J.R., and Crowley, J. Transplantation system for determining the clonogenic survival of parenchymal hepatocytes exposed to ionizing radiation. Cancer Res **41,** 3512, 1981.
36. Chandrasekaran, P., Seagle, C., Rice, L., Macdonald, J., and Gerber, D.A. Functional analysis of encapsulated hepatic progenitor cells. Tissue Eng **12,** 2001, 2006.
37. Winnike, J.H., Pediaditakis, P., Wolak, J.E., McClelland, R.E., Watkins, P., and Macdonald, J.M. Stable isotope resolved

metabolomics of primary human hepatocytes reveals a stressed phenotype. Metabolomics **8,** 34, 2012.
38. Masson, S., and Quistorff, B. The phosphorous-31 NMR visibility of ATP in perfused rat liver remains about 90%, unaffected by changes of metabolic state. Biochemistry **31,** 7488, 1992.
39. Macdonald, J.M., Schmidlin, O., and James, T.L. *In vivo* monitoring of hepatic glutathione in anesthetized rats by 13C NMR. Magn Reson Med **48,** 430, 2002.
40. Joly, A., Desjardins, J.F., Fremond, B., Desille, M., Campion, J.P., Malledant, Y., *et al.* Survival, proliferation, and functions of porcine hepatocytes encapsulated in coated alginate beads: a step toward a reliable bioartificial liver. Transplantation **63,** 795, 1997.
41. Irani, K., Pomerantseva, I., Hart, A.R., Sundback, C.A., Neville, C.M., and Vacanti, J.P. Mechanical dissociation of swine liver to produce organoid units for tissue engineering and *in vitro* disease modeling. Artif Organs **34,** 75, 2010.
42. Amimoto, N., Mizumoto, H., Nakazawa, K., Ijima, H., Funatsu, K., and Kajiwara, T. Hepatic differentiation of mouse embryonic stem cells and induced pluripotent stem cells during organoid formation in hollow fibers. Tissue Eng Pt A **17,** 2071, 2011.
43. Glicklis, R., Merchuk, J.C., and Cohen, S.M. Modeling mass transfer in hepatocyte spheroids via cell viability, spheroid size, and hepatocellular functions. Biotechnol Bioeng **86,** 672, 2004.
44. McClelland, R.E., and Coger, R.N. Use of micropathways to improve oxygen transport in a hepatic system. J Biomech Eng **122,** 268, 2000.
45. Jungermann, K. Metabolic zonation of liver parenchyma. Semin Liver Dis **8,** 329, 1988.
46. Sulieman, S.A., and Stevens, J.B. The effect of oxygen tension on rat hepatocytes in short-term culture. In Vitro Cell Dev Biol **23,** 332, 1987.
47. Wölfle, D., and Jungermann, K. Long-term effects of physiological oxygen concentrations on glycolysis and gluconeogenesis in hepatocyte cultures. Eur J Biochem **151,** 299, 1985.
48. Fariss, M.W. Oxygen toxicity: unique cytoprotective properties of vitamin E succinate in hepatocytes. Free Radic Biol Med **9,** 333, 1990.
49. Motoyama, S., Saito, S., Inaba, H., Kitamura, M., Minamiya, Y., Suziki, H., *et al.* Red blood cells attenuate sinusoidal endothelial cell injury by scavenging xanthine oxidase-dependent hydrogen peroxide in hyperoxic perfused rat liver. Liver **20,** 200, 2000.
50. Rotem, A., Toner, M., Tompkins, R.G., and Yarmush, M.L. Oxygen uptake rates in cultured rat hepatocytes. Biotechnol Bioeng **40,** 1286, 1992.
51. Comar, J.F., Suzuki-Kemmelmeier, F., Constantin, J., and Bracht, A. Hepatic zonation of carbon and nitrogen fluxes derived from glutamine and ammonia transformations. J Biomed Sci **17,** 1, 2010.
52. Wurm, M., Woess, C., Libiseller, K., Beer, B., and Pavlic, M. Challenging small human hepatocytes with opiates: further characterization of a novel prototype bioartificial liver. Tissue Eng Part A **16,** 807, 2010.
53. Jungermann, K., and Kietzman, T. Role of oxygen in the zonation of carbohydrate metabolism and gene expression in liver. Kidney Int **51,** 402, 1997.
54. Garber, K. Energy boost: the Warburg effect returns in a new theory of cancer. J Natl Cancer Inst **96,** 1805, 2004.

Address correspondence to:
Jeffrey M. Macdonald, PhD
Department of Biomedical Engineering
University of North Carolina at Chapel Hill
Chapel Hill, NC 27599-7575

E-mail: jmacdona@med.unc.edu

Received: November 6, 2011
Accepted: June 28, 2012
Online Publication Date: October 1, 2012